Distribution of Time-Energy Entanglement over 100 km fiber using superconducting single-photon detectors

Qiang Zhang[1], Hiroki Takesue[2], Sae Woo Nam[3], Carsten Langrock[1], Xiuping Xie[1], Burm Baek[3], M. M. Fejer[1], and Yoshihisa Yamamoto[1,4]

[1] Edward L. Ginzton Laboratory, Stanford University, Stanford, California 94305
[2] NTT Basic Research Laboratories, NTT Corporation, 3-1 Morinosato Wakamiya, Atsugi, Kanagawa 243-0198, Japan
[3] National Institute of Standards and Technology, 325 Broadway, Boulder, Colorado 80305
[4]National Institute of Informatics, 2-1-2 Hitotsubashi, Chiyoda-ku, Tokyo, 101-843, Japan
qiangzh@stanford.edu

Abstract: In this letter, we report an experimental realization of distributing entangled photon pairs over 100 km of dispersion-shifted fiber. In the experiment, we used a periodically poled lithium niobate waveguide to generate the time-energy entanglement and superconducting single-photon detectors to detect the photon pairs after 100 km. We also demonstrate that the distributed photon pairs can still be useful for quantum key distribution and other quantum communication tasks.

OCIS codes: (190.4410) Nonlinear optics, parametric processes; (230.7380) Waveguides, channeled.

References and links

1. A. K. Ekert, "Quantum cryptography based on Bell's theorem," Phys. Rev. Lett. **67**, 661-663 (1991).
2. N. Gisin, G. Ribordy, W. Tittel, and H. Zbinden, "Quantum Cryptography," Rev. Mod. Phys, **74**, 145 (2002).
3. I. Marcikic, H. de Ridmatten, W. Tittel, H. Zbinden, and N. Gisin, "Long distance teleportation of qubits at teclecommunication wavelengths," Nature **421**, 509 (2003).
4. R. Ursin, T. Jennewein, M. Aspelmeyer, R. Kaltenbaek, M. Lindenthal, P. Walther, and A. Zeilinger, "Quantum teleportation across the Danube," Nature **430**, 849 (2004).
5. C.–Z. Peng, T. Yang, X.–H. Bao, J. Zhang, X.-M. Jin, F.-Y. Feng, B. Yang, J. Yang, J. Yin, Q. Zhang, N. Li, B.-L. Tian, and J.-W. Pan, "Experimental free-space distribution of entangled Photon pairs over 13 km: towards satilite-based global quantum communication," Phys. Rev. Lett. **94**, 150501 (2005);
6. R. Ursin, F. Tiefenbacher, T. Schmitt-manderbach, H. Weier, T. Scheidl, M. Lindenthai, B. Blauensteiner, T. Jennewein, J. Perdigues, P. Trojek, B. Ömer, M. Furst, M. Meyenburg, J. Rarity, Z. Sodnik, C. Barbieri, H. Weinfurter, and A. Zeilinger, "Entanglement-based quantum communication over 144km," Nat. Phys. **3,** 481 (2007).
7. I. Marcikic, H. de Riedmatten,W. Tittel, H. Zbinden,M. Legre, and N. Gisin, "Distribution of time-bin entangled qubits over 50 km of optical fiber," Phys. Rev. Lett. **93**, 180502 (2004).
8. H. Takesue, "Long-distance distribution of time-bin entanglement generated in a cooled fiber," Opt. Express **14**, 3453 (2006).
9. T. Honjo, H. Takesue, H. Kamada, Y. Nishida, O. Tadanaga, M. Asobe, and K. Inoue, "Long-distance distribution of time-bin entangled photon pairs over 100 km using frequency up-conversion detectors," Opt. Express 15, 13957 (2007).
10. C. Liang, K. F. Lee, J. Chen, and P. Kumar, "Distribution of fiber-generated polarization entangled photon-pairs over 100 km of standard fiber in OC-192WDMenvironment," postdeadline paper, Optical Fiber Communications Conference (OFC2006), paper PDP35.
11. H. Hübel, M. Vanner, T. Lederer, B. Blauensteiner, T. Lorünser, A. Poppe, and A. Zeilinger, "High-fidelity transmission of polarization encoded qubits from an entangled source over 100 km of fiber," Opt. Express **15,** 7853, (2007).
12. J. D. Franson, "Bell inequality for position and time," Phys. Rev. Lett. **62**, 2205 (1989).
13. G. N. Gol'tsman, O. Okunev, G. Chulkova, A. Lipatov, A. Semenov, K. Smironov, B. Voronov, A. Dzardanov, C. Williams, and R. Sobolewski, "Picosecond superconducting single-photon optical detector," Appl. Phys. Lett. **79**, 705 (2001).
14. R. Hadfield, M. Stevens, S. Gruber, A. Miller, R. Schwall, R. Mirin, and S.-W. Nam, "Single photon source characterization with a superconducting single photon detector," Opt. Express **13**, 10846-10853 (2005).

#91197 - $15.00 USD Received 2 Jan 2008; revised 17 Feb 2008; accepted 27 Feb 2008; published 10 Apr 2008

15. K. Parameswaran, R. Route, J. Kurz, R. Roussev, M. Fejer and M. Fujimura, "Highly efficient second-harmonic generation in buried waveguides formed by annealed and reverse proton exchange in periodically poled lithium niobate," Opt. Lett. **27**, 179 (2002).
16. I. Ali-Khan, C. J. Broadbent, and J. C. Howell, "Large-alphabet QKD using energy-time entangled bipartite states," Phys. Rev. Lett. **98**, 060503 (2007).
17. X. Xie and M. M. Fejer, "Two-spatial-mode parametric amplifier in lithium niobate waveguides with asymmetric Y junctions," Opt. Lett. **31**, 799-801 (2006).
18. Q. Zhang, X. Xie, H. Takesue, S. W. Nam, C. Langrock, M. M. Fejer, and Y. Yamamoto, "Correlated photon-pair generation in reverse-proton-exchange PPLN waveguide with integrated mode demultiplexer at 10 GHz clock," Opt. Express **15**, 10288 (2007).
19. G. P. Agrawal, *Nonlinear Fiber Optics*, (Academic Press, 1995), pp. 60-87.
20. T. Honjo, K. Inoue, and H. Takahashi, "Differential-phase-shift quantum key distribution experiment with a planar light-wave circuit Mach–Zehnder interferometer," Opt. Lett. **29**, 2797 (2004)
21. J. F. Clauser, M. Horne, A. Shimony, and R. A. Holt, "Proposed experiment to test local hidden-variable theories," Phys. Rev. Lett. **23**, 880-884 (1996).

1. Introduction

Entanglement distribution is one of the core components in the field of long-distance quantum communication (LDQC), for example, quantum key distribution (QKD) [1, 2] and quantum teleportation [3,4]. So far there are many experimental implementations of entanglement distribution over free-space links [5, 6], or optical fibers [7-11].

Time-energy-entangled photon pairs [12] at telecom wavelengths are thought to be good candidates for LDQC over fiber-based networks [7-9], because it has low propagation loss in standard optical fiber and insensitivity to polarization-mode dispersion compared with polarization-entangled photon pairs.

Very recently, 100-km entanglement distribution over optical fiber has been reported by several groups [9-11]. Longer distances are currently limited by the detectors' dark count rates (DCRs) and timing resolution. Superconducting single-photon detectors (SSPDs) [13,14] provide very low DCRs and low jitter. Here, we combined two SSPDs (<200 Hz DCR and 65 ps full-width-at-half-maximum jitter) and a reverse-proton-exchange (RPE) periodically poled lithium niobate (PPLN) waveguide to generate and distribute entangled photon pairs over 100 km of dispersion-shifted fiber (DSF). The low DCRs and jitter of these SSPDs reduce the number of accidental coincidences. RPE PPLN waveguides [15] were used due to their high nonlinear efficiencies and low propagation loss (<0.1 dB/cm). We demonstrated that the entanglement after 100 km still showed quantum nonlocality and violated Bell's inequality by observing the two-photon-interference fringes.

2. Time-energy entanglement

As shown in Fig. 1, a continuous-wave laser with an ultra-long coherence time τ_1 pumps a crystal possessing a $\chi^{(2)}$ nonlinearity, generating correlated photon pairs via the parametric down conversion (PDC) process. The down-converted photon pairs usually have a much broader spectrum than the pump photons and hence a significantly shorter coherence time τ_2 according to the time-bandwidth limit. Since the two photons of a photon pair are always generated simultaneously and the down conversion process obeys energy conservation, both the total energy and the time difference of the two photons are well defined as the pump photon's energy and zero, respectively. However, we do not know the exact time and energy of each photon. The state can be mathematically expressed as, $\left|\psi\right\rangle = C\int dt_1 dt_2 e^{-(t_1-t_2)^2/4\tau_2^2} e^{-(t_1+t_2)^2/16\tau_1^2} e^{-i(\omega_p/2)(t_1+t_2)} a_1^+(t_1)a_2^+(t_2)\left|0\right\rangle$, where C is a normalization constant, w_p is the frequency of the pump photons and $a_i^+(t_i)$ is the photon creation operator in mode i at time t_i [16]. These types of entanglement have been widely used for testing of quantum nonlocality and quantum key distribution.

#91197 - $15.00 USD Received 2 Jan 2008; revised 17 Feb 2008; accepted 27 Feb 2008; published 10 Apr 2008

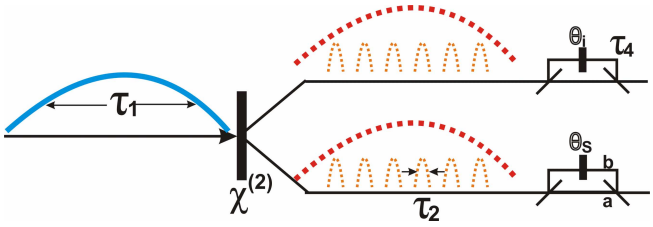

Fig. 1. Scheme for generation and detection of time-energy entanglement. The small dotted pulses represent the possible photon pairs, which can be generated during the long time span of the pump light, while the dotted red envelope of the photon pairs is from the long pump.

To characterize and utilize time-energy entanglement, one usually launches the entangled photon pairs into two unbalanced Mach-Zehnder interferometers (MZI) and then implements a coincidence measurement by detecting the outputs of the two MZIs using single-photon detectors. We define the timing jitter of the single-photon detector as τ_3 and the time unbalance between the MZI's two paths as τ_4. Suppose that $\tau_1 >> \tau_4 > \tau_2, \tau_3$, so that there will be no single-photon coherence fringe in the MZI's output and a two-photon interference pattern will be observed with a coincidence measurement. The phase of the MZI's long arm can be adjusted to choose the measurement basis. For example, the signal channel's measurement basis is $|a\rangle_s + e^{i\theta_s}|b\rangle_s$, where θ_s is the signal channel's phase and a, b are the MZI's two arms, respectively. When θ_s is changed in the experiment, the state vector of the measurement basis rotates along the equator of the Poincaré sphere.

The interference pattern can be estimated as ~ $1+V\cos(\theta_s+\theta_i-2\omega\tau_4)$, where V is the visibility of the interference fringes, and ω denotes the angular frequency of the pump light. The visibility estimated with the following formula:

$$V=\frac{\mu\eta_{ch}^2\eta_d^2}{\mu\eta_{ch}^2\eta_d^2+2\mu^2\eta_{ch}^2\eta_d^2+8\mu\eta_{ch}\eta_d Dt+8D^2t^2+\zeta\mu\eta_{ch}^2\eta_d^2} \quad (1)$$

where μ is average photon pair number per time window, η_{ch} is the channel loss, η_d is the detector's quantum efficiency, Dt is probability of a dark count in time window t, and ζ is the imperfection of the MZI. The numerator of the Eq. (1) represents the coincidence due to the entanglement. Since the pump coherence time τ_1 is much longer than the photon pairs' coherence time τ_2, the photon pairs follow a Poissionian distribution with the second term in the denominator of Eq. (1) representing the contribution of multi-photon pair generation. The third and forth item in the denominator represents the accidental coincidence by the dark counts and the photon pairs. The last item in the denominator is the accidental coincidence by the imperfection of the MZIs. From Eq. (1) we can see that when the channel loss increases with the transmission distance, the third and forth items in the denominator become bigger compared with other items, i. e. the dark count rates per time window contributes more to the reduction of visibility.

3. Experimental setup

A tunable external cavity diode laser with 100 kHz linewidth was used to generate the pump light for the PDC process. The center wavelength of the laser was tuned to 1559 nm with a full-width-at-half-maximum (FWHM) coherence time of 4 μs. The output of the laser was amplified by two erbium-doped fiber amplifiers (EDFAs) and then launched into a RPE PPLN

#91197 - $15.00 USD Received 2 Jan 2008; revised 17 Feb 2008; accepted 27 Feb 2008; published 10 Apr 2008

waveguide to generate frequency-doubled pump light for the PDC process via second harmonic generation (SHG) as shown in Fig. 2. One 3-nm-wide tunable bandpass filter was inserted after each EDFA, respectively, to remove the EDFAs' spontaneous emission noise. Because the waveguide devices used only accept TM-polarized light, an in-line fiber polarization controller was used to adjust the polarization state of the input. The residual pump photons after the second harmonic generation was attenuated by 180 dB using dichroic mirrors and pump filters. The second-harmonic (SH) wave was then launched into a second RPE PPLN waveguide to serve as the pump pulse for the PDC process.

Since RPE PPLN waveguides fabricated on z-cut substrates only support TM-polarized waves, separation of the near degenerate signal and idler waves via polarization de-multiplexing is not possible. To solve the problem, we use higher-order-mode interactions in combination with integrated mode multiplexers / demultiplexers via asymmetric Y-junctions to separate the signal and idler photons [17, 18].

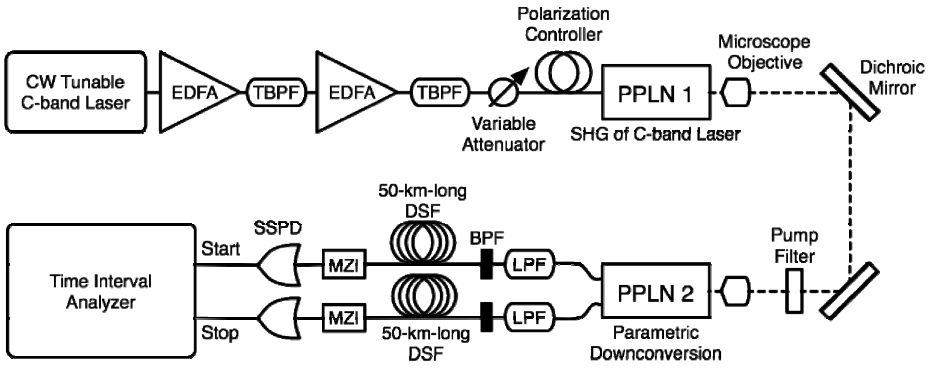

Fig. 2. Diagram of the experimental setup. TBPF: tunable band-pass filter. PPLN1: a RPE PPLN waveguide for second harmonic generation of the pump source. PPLN2: a fiber pigtailed asymmetric Y-junction RPE PPLN waveguide for parametric down-conversion. LPF: long-pass filter to remove the 780 nm pump light and other parasitics. BPF: 0.8-nm-wide bandpass filter. SSPD: superconducting single-photon detector. TIA: time interval analyzer. Solid lines represent optical fibers and dotted lines represent free-space propagation.

The generated entangled photon pairs and residual pump light were collected at the output of the RPE PPLN waveguide via a fiber pigtail. The spectral bandwidth of the entangled photon pairs was approximately 40 nm [17]. A long-pass filter was inserted into each output fiber of the second RPE PPLN chip to eliminate the residual pump light (second harmonic photons) as well as other fluorescence components. The photon pairs were then input into two spools of 50-km-long DSF, respectively. Two 0.8-nm-wide bandpass filters were inserted before the fiber spools to reduce the bandwidth of the photon pairs, limiting the total dispersion that will be accumulated after the photons are coupled into the long spools of DSF. The band-pass filter also defined the photon pairs' time duration to be 4 ps (FWHM). The chromatic dispersion in the 100 km fiber broadened the photon pairs' pulse duration from 4 ps to 25 ps [19]. The 25 ps time duration was still smaller than the timing jitter of the SSPD and would not reduce the visibility.

The entangled photon pairs were analyzed by two 10-GHz unbalanced planar lightwave circuit (PLC) MZIs. The phase between the two arms of the MZIs could be controlled by adjusting the temperature of the interferometer using a Peltier element [20]. The time difference between the two arms was 100 ps, i.e. $\tau_4 = 100\,ps$, meeting the condition $\tau_1 >> \tau_4 > \tau_2$. Therefore, one observes the two-photon-coincidence condition and not the single photon interference. The extinction ratio of the MZIs was ~20 dB so $\zeta \sim 0.01$.

#91197 - $15.00 USD Received 2 Jan 2008; revised 17 Feb 2008; accepted 27 Feb 2008; published 10 Apr 2008

As shown in Eq. (1), low DCR and narrow time window will reduce the accidental coincidence by the dark count, which is the main distribution to the reduction of the visibility at longer distance transmission. In order to narrow time window but still keep the count rate, we need a low jitter detector. In our experiment, we used two SSPDs to detect the entangled photon pairs. The SSPDs used in our experiment consisted of a 100-nm-wide, 4-nm-thick NbN superconducting wire, which was coupled to a 9-μm core single-mode fiber [13]. The packaged detectors were housed in a closed-cycle cryogen-free refrigerator with an operating temperature of 3 K. The quantum efficiency and dark count rate of the SSPDs depended on an adjustable bias current. In the experiment, we set the bias current to reach a quantum efficiency of 0.7% and 2.1% for the signal and idler channel, respectively, and a dark count rate of around 100 Hz. These SSPDs had an inherently small Gaussian timing jitter of 65 ps (FWHM). In the experiment, we set our coincidence time window to 100 ps. Therefore, the dark count propability per time window was 10^{-8}, which reduced the accidental coincidence rate caused by dark counts compared to previous experiments [7-9].

The detected signals were sent to a time interval analyzer (TIA) whose timing response was also faster than τ_4 to measure the time coincidence histogram. The signal channel detection event was used as the start and the idler channel as the stop signal.

4. Experimental results

In the experiment, we input 316 mW of pump at a wavelength of 1559 nm into the first PPLN waveguide from the EDFA and coupled 560 μW of the generated SH into the second PPLN chip.

We set the time window to 100 ps (τ_3), which was a bit larger than the timing jitter of the SSPD to eliminate the timing fluctuations caused by temperature and polarization instabilities. Under these condition, we achieved 0.08 average photon pairs per time window. The total channel loss before the 100-km-long fiber was 20 dB, with 10 dB due to the PPLN's propagation, reflection, scattering and fiber pigtailing loss, and 10 dB losses from the filters. Each of the two PLC MZIs had a 5 dB insertion loss.

Using the above data of channel loss, we can estimate the theoretical visibility without additional fiber transmission to be 85.5%, assuming the following parameters for the contributions due to multi-photon pairs, imperfections of the MZIs and the accidental coincidence by detectors' dark-count rates, 13.6%, 0.8% and 0.017%, respectively. Due to their smallness, the detectors' DCRs can be ignored. To confirm our theory about the visibility and demonstration of the entanglement, we took a back-to-back coincidence measurement of the interference pattern without any additional fiber spans. We first set the PLC interferometer's temperature in the signal channel to 22.5°C and varied the temperature of the interferometer in the idler channel to change its phase and obtain a two-photon-coincidence interference-fringe pattern. To demonstrate entanglement, one interference pattern is not enough; at least one other pattern for the signal channel in a non-orthogonal basis is necessary. To observe the pattern in another non-orthogonal basis, we changed the signal interferometer temperature to 24.5°C and observed the interference fringes shown in Fig. 4(a). The average experimentally achieved visibility was $(83.58 \pm 0.05)\%$, which was similar to our theoretical estimate 85%.

The DSF's loss was 0.2 dB/km, resulting in a 20 dB channel loss after 100 km of fiber. According to Eq. (1), the dark counts' contribution to the denominator is now 0.17%, which still can be ignored and only reduced the theoretical visibility from 85.5% to 85.3%. For comparison, using a commercially available InGaAs or up-conversion-based detector with our entanglement source with higher quantum efficiency but larger DCR [7-9], the visibility would be reduced to 70%. Thus the utilization of SSPDs in our setup helps to improve the visibility at longer distance.

#91197 - $15.00 USD Received 2 Jan 2008; revised 17 Feb 2008; accepted 27 Feb 2008; published 10 Apr 2008

We performed an identical coincidence measurement after 100 km of DSF. The two observed curves shown in Fig. 4(b) have an average visibility of $(80.5 \pm 7)\%$, which is beyond the 71% visibility necessary for violation of the Bell inequality [21], and hence demonstration of entanglement. The large uncertainty of the visibility resulted from system instabilities, for example, temperature fluctuations of the two PPLN chips, the polarization and timing fluctuations caused by the temperature change of the 100-km-long fiber, etc. In the experiment, it took several hours to take each curve in Fig. 4(b) due to the low flux of entangled photon pairs. The long measurement time accentuated polarization and timing fluctuations between the two measurements, and is also the reason for the different heights of the two curves in the figure. Including all the channel loss terms, we obtained entangled photon pairs at a 2 Hz rate after 100 km of propagation.

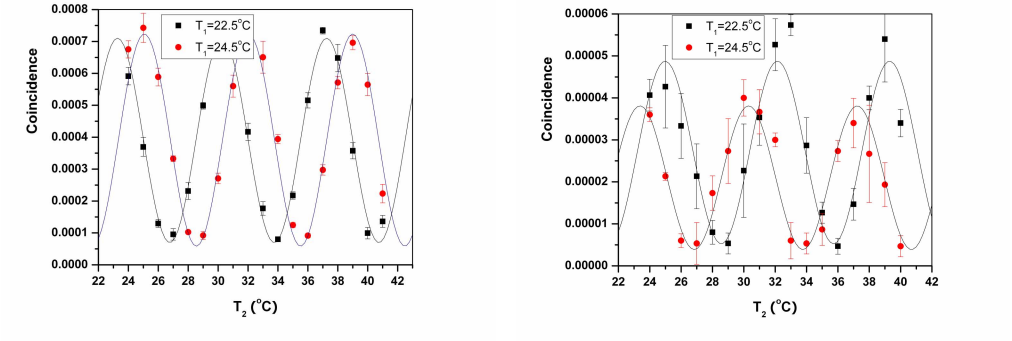

(a) (b)

Fig. 4. Two-photon interference pattern (a) without and (b) with 100-km-long fiber (b). T_1 is the temperature of the PLC MZI in the signal channel while T_2 is the temperature in the idler channel. The Y-axis represents the coincidence rate per signal photon with an average of 0.5 million signal photons.

5. Conclusion

We experimentally generated and distributed time-energy entanglement at telecom wavelengths with a RPE PPLN waveguide over a 100-km-long dispersion shifted fiber with the help of SSPDs. The visibility of the achieved entanglement was $(80.5 \pm 7)\%$ without subtracting any noise when the entanglement flux was 2 Hz, which can be used in quantum key distribution. With improvement of our waveguide and filtering loss, we can extend our entanglement distribution to longer distances using SSPDs.

Acknowledgment

This research was supported by NICT, the U.S. Air Force Office of Scientific Research through contracts F49620-02-1-0240, the MURI center for photonic quantum information systems (ARO/ARDA program DAAD19-03-1-0199), the Disruptive Technology Office (DTO), SORST, and CREST programs, Japan Science and Technology Agency (JST) and the NIST quantum information science initiative. We acknowledge the support of Crystal Technology, Inc.

#91197 - $15.00 USD Received 2 Jan 2008; revised 17 Feb 2008; accepted 27 Feb 2008; published 10 Apr 2008